

Resveratrol ameliorates oxaliplatin-induced neuropathic pain via anti-inflammatory effects in rats

ZHI-BIN DONG^{1*}, YU-JIA WANG^{2*}, WEN-JUN WAN^{3*}, JI WU⁴,
BO-JUN WANG⁵, HAI-LI ZHU⁵, MIN XIE⁵ and LING LIU⁵

¹School of Pharmacy, Xianning Medical College, Hubei University of Science and Technology;

²Xianning Central Hospital, The First Affiliated Hospital of Hubei University of Science and Technology,

Xianning, Hubei 437100; ³Xishui Hospital Affiliated to Hubei Institute of Science and Technology, Huanggang,

Hubei 438299; ⁴Department of Neurosurgery, Affiliated Hospital of Youjiang Medical University for Nationalities,

Baise, Guangxi Zhuang Autonomous Region 531412; ⁵School of Basic Medical Sciences, Xianning Medical College,

Hubei University of Science and Technology, Xianning, Hubei 437100, P.R. China

Received April 2, 2022; Accepted June 28, 2022

DOI: 10.3892/etm.2022.11523

Abstract. Oxaliplatin (OXA) is a common chemotherapy drug and exhibits clinical activity in several cancer types. Its anticancer clinical effect is frequently accompanied by neurotoxicity. The symptoms include paresthesia and pain, which adversely affect the quality of life of patients. In the present study, five consecutive intraperitoneal injections of 4 mg/kg OXA were used to mimic chemotherapy in rats. OXA administration induced mechanical allodynia, activated spinal astrocytes and triggered the inflammatory response. To explore potential therapeutic options for OXA-induced neuropathic pain, resveratrol (Res) was intrathecally injected into the spinal cord of OXA-treated rats. Paw withdrawal threshold values of OXA-treated rats were increased, indicating an antinociception effect of Res on OXA-induced pain. Additionally, Res treatment reduced the levels of glial fibrillary acidic protein, TNF- α , IL-1 β and NF- κ B, which were upregulated in OXA-treated rats (compared with control). Furthermore, Auto Dock data showed that Res binds to cyclooxygenase-2 (COX-2) through six hydrogen bonds. Western blot analysis and reactive oxygen species (ROS) assays indicated that Res treatment decreased COX-2 expression and suppressed ROS production. In summary, intrathecal injection of Res reduced the spinal COX-2-mediated ROS generation and inflammatory reaction,

suppressed astrocytic activation, and alleviated OXA-induced neuropathic pain.

Introduction

Oxaliplatin (OXA) is a third-generation platinum-based chemotherapeutic drug, which has a broad spectrum of anticancer activity (1). With the increasing clinical application of OXA, inevitable adverse reactions have been reported (2). Peripheral neuropathic pain is the major side effect affecting 85-90% of patients following OXA treatment and this can last for months or years (3,4). In clinical practice, all types of analgesics have little effect in mitigating this type of pain (5,6). Severe neuropathic pain may lead to dose reduction or even discontinuation of OXA chemotherapy, which is unfavorable for tumor control and survival (7). Therefore, the study of the pathological mechanism of OXA-induced neuropathy and the development of related analgesics have important clinical significance.

The spinal cord is involved in the processing of nociceptive information by receiving and integrating information from the peripheral nervous system and transmitting this information to the brain (8). OXA may induce pathophysiological changes in the spinal cord, including the release of pro-inflammatory cytokines and increase of oxidative stress (9). Pro-inflammatory cytokines are mainly released by activated astrocytes (10). During the development of pain, astrocytes become reactive and last longer and undergo hyperplasia and hypertrophy within several days after injury (11). Activated astrocytes release numerous pro-inflammatory mediators and activate intracellular signaling to maintain the pain process (12). The increased oxidative stress activates a variety of transcription factors, leading to the differential expression of genes involved in inflammatory pathways and triggering the inflammatory response (13). Therefore, the inhibition of the inflammatory response mediated by activated astrocytes and the increased oxidative stress can be potential therapeutic targets for the treatment of OXA-induced neuropathic pain.

Correspondence to: Dr Ling Liu, School of Basic Medical Sciences, Xianning Medical College, Hubei University of Science and Technology, 88 Xianning Avenue, Xian'an, Xianning, Hubei 437100, P.R. China
E-mail: liuling0306@163.com

*Contributed equally

Key words: oxaliplatin-induced neuropathic pain, spinal inflammation, resveratrol, cyclooxygenase-2

Resveratrol (Res) is a natural polyphenolic flavonoid, which has antioxidative, anticancer and antiproliferative effects (14). Although Res has multiple beneficial effects, it induces harmful effects at high concentration, such as pro-oxidant effect (15). However, low dose administration of Res (1 mg/kg) did not adversely affect animals' health (16). Res has been reported to be a powerful antioxidant with remarkable anti-inflammatory properties (17). Furthermore, a pre-clinical study has demonstrated that Res has a beneficial effect on the management of pathological pain (18). In a neuropathic mouse model of chronic constriction injury of the sciatic nerve, Res treatment repressed the expression of pro-inflammatory cytokines, including TNF- α , IL-1 β and IL-6 (19). In a complete Freund's adjuvant-induced joint inflammatory pain C57BL/6 mouse model, Res treatment reduced the spinal cord expression of NF- κ B, TNF- α and IL-1 β , and alleviated inflammatory pain (18). In a spared nerve injury rat model, Res suppressed microglia-mediated neuroinflammation and relieved neuropathic pain (20). In line with these findings, a previous study has demonstrated that Res can alleviate bone cancer pain (19). The present study aimed to investigate the effect and the mechanism of action of Res on OXA-induced pathological pain.

Materials and methods

Animals and drug administration. A total of 36 Male Sprague-Dawley rats weighing 180-200 g (6-8 weeks old) were purchased from Hubei Province Experimental Animal Center. Animals were housed in a temperature-controlled room (22 \pm 1 $^{\circ}$ C) and 55 \pm 5% humidity with a 12/12 h light-dark cycle regime and access to water and food *ad libitum*. All efforts were made to minimize the number of animals used and their suffering.

OXA (Selleck Chemicals) was dissolved in 5% glucose solution (21). Res (3,5,40-trihydroxystilbene; Sigma-Aldrich; Merck KGaA) was dissolved in DMSO and diluted with 0.9% NaCl. Rats were randomly divided into four groups: Control, Res, OXA and OXA + Res. Each group contained six rats. For OXA treatment, the rats from the OXA and OXA + Res groups received intraperitoneal injection of 4 mg/kg OXA once daily for 5 consecutive days. The rats from the Control and Res groups received intraperitoneal injection of the same volume of 5% glucose solution once daily for 5 consecutive days. The pain behavioral test was performed 6 days after the first OXA injection. At 7 days after the first OXA injection, the rats from the Res and OXA + Res groups were intrathecally injected with Res (1 mg/kg). The Control and OXA groups were intrathecally injected with the same volume of vehicle (DMSO and 0.9% NaCl). Intrathecal injection was performed as previously described (22,23). Briefly, rats were anesthetized through an intraperitoneal injection of 50 mg/kg sodium pentobarbital and the skin was sterilized with 75% alcohol. Then, a 25- μ l Hamilton syringe with a 30-gauge needle was held at an angle of \sim 20 $^{\circ}$ above the vertebral column. The needle was inserted into the intervertebral space between L5 and L6. A puncture stimulating a tail-flick reaction was considered as successful. The Res solution (10 μ l) was injected and the needle was left in the dosing position for >30 sec after injection. Subsequently, the mechanical allodynia assay was performed at 0, 2, 4 and 6 h after Res administration.

Antibodies and reagents. Anti-NF- κ B p65 mouse monoclonal antibody (cat. no. BF8005) and β -actin rabbit antibody (cat. no. AF7018) were obtained from Affinity Biosciences. GFAP rabbit polyclonal antibody (cat. no. A0237), IL-1 β rabbit monoclonal antibody (cat. no. A19635), TNF- α rabbit polyclonal antibody (cat. no. A0277) and COX-2 rabbit polyclonal antibody (cat. no. A1253) were purchased from ABclonal Biotech Co., Ltd.. The Reactive Oxygen Species Assay kit (cat. no. S0033S) and Mito-Tracker Red CMXRos (C1049B) were obtained from Beyotime Biotechnology. H&E staining solution (cat. no. BL735B) was purchased from Biosharp Life Sciences. Res (cat. no. 501-36-0) was purchased from Sigma. OXA (cat. no. 61825-94-3) was obtained from Shanghai Aladdin Biochemical Technology Co., Ltd. The secondary antibodies used for western blotting were HRP Goat Anti-Rabbit IgG (H+L) (AS014) and HRP Goat Anti-Mouse IgG (H+L) (AS014), purchased from ABclonal Technology. The secondary antibodies used for immunofluorescence analysis were Goat anti-mouse IgG H&L (FITC) (ab6785), Goat Anti-Rabbit IgG H&L (TRITC; cat. no. ab6718) and Goat Anti-Rabbit IgG H&L (FITC) (ab6717), purchased from Abcam.

Mechanical allodynia assay. The paw withdrawal threshold (PWT) was determined using the modified up-down method (24). Rats were accustomed individually for 30 min in a transparent plastic box with a 5x5 cm wire mesh grid floor. Subsequently, the von Frey filaments (0.4-26 g; Stoelting Co.) were used to stimulate the hind paw. The filaments were pressed vertically against the mid-plantar surface of the hind paw. The force caused filaments bent and this state was maintained for 3-5 s with a 2-min interval between two stimulations. A positive response was defined as paw withdrawal was observed within 3 sec of the stimulated hind paw. Six measurements were taken for each rat. If a positive response was obtained, a lower level of von Frey hair was used; conversely, the next higher force was used. The pattern of the positive and negative withdrawal response was converted to PWT. After the behavioral test, three rats were perfused and fixed for morphological analysis, including H&E staining and immunofluorescence. The other three rats were sacrificed and the spinal cord were collected for western blot analysis.

Cell culture and Res treatment. C6 glial cells (Jennio Biotech Co., Ltd.) were cultured in DMEM supplemented with 10% fetal bovine serum, 50 U/ml penicillin and 50 μ g/ml streptomycin (all Gibco; Thermo Fisher Scientific, Inc.) at 37 $^{\circ}$ C with 5% CO $_2$. For ROS and mitochondrial membrane potential assessment, C6 glial cells (1.5x10 5) were seeded on a 24-well plate and incubation with 5 ng/ μ l TNF- α at 37 $^{\circ}$ C for 4 h. Subsequently, cells were treated with 0 and 1 μ M Res at 37 $^{\circ}$ C for 24 h and then the cells were used for ROS assessment and mitochondrial membrane potential detection. TNF- α was diluted with 0.9% NaCl. Res was dissolved in DMSO (Beyotime Biotechnology).

H&E staining. After 5 days of OXA administration and subsequent Res treatment, the rats from the Control, OXA and OXA + Res groups (n=3/group) were deeply anesthetized with 60 mg/kg sodium pentobarbital and perfused

transcardially with saline containing heparin. The clearing of the liver (red to light brown in color) is an indicator of a good perfusion. Then switched perfusate to 4% paraformaldehyde (PFA, 0.1 M phosphate buffer, pH 7.4) and perfused until the animal body was stiff and rigid. After perfusion was complete, spinal cords were removed and post-fixed in 4% PFA (0.1 M phosphate buffer, pH 7.4) for 12 h at 4°C and embedded in paraffin. Subsequently, the tissues were cut into 4- μ m sections using a microtome (RM 2165; Leica Microsystems GmbH). The sections were stained using the standard H&E method. Briefly, paraffin sections were treated with xylene (5 min, two times), 100% ethanol (10 min, two times), 90% ethanol (10 min), 70% ethanol (10 min) for dewaxing and rinsing with tap water for 2 min. Then the sections were dyed with hematoxylin solution for 3 min and washed with tap water for 10 sec. The sections were stained with eosin for 3 min and washed with tap water for 10 sec. The dehydration and transparent treatment were conducted by putting the slices into 80% ethanol (5 min), 90% ethanol (5 min), 95% ethanol (5 min), 100% ethanol (5 min, two times), xylene (5 min, times). Finally, the sections were sealed with neutral balsam and observed using a fluorescence microscope (Olympus IX73; Olympus). H&E images were analyzed using the ImageJ 1.51j8 software (National Institutes of Health). The scoring criteria of inflammation cell infiltration (25) is: 0 (normal); 1 (lymphocyte infiltration around meninges and blood vessels); 2, 1-10 lymphocytes in a field); 3 (11-100 lymphocytes in a field); 4 (>100 lymphocytes in a field).

Immunofluorescence analysis. For immunofluorescence analysis, the paraffin sections were treated with xylene (5 min, two times), 100% ethanol (10 min, two times), 90% ethanol (10 min), 70% ethanol (10 min) for dewaxing and rinsing with ddH₂O (5 min, two times). Then the sections were conducted to antigen retrieval (Improved Citrate Antigen Retrieval Solution, P0083, Beyotime Biotechnology). Immerse the slices in antigen retrieval solution and heat at 95-100°C for 20 min. The antigen retrieval solution was preheated to 95-100°C before use. Then cooled to room temperature and washed 1-2 times with distilled water for 3-5 min. After incubation with 3% hydrogen peroxide for 10 min, immunostaining was performed. The tissue sections were blocked with goat serum (Gibco, 10%, room temperature) for 1 h and then incubated with primary antibody overnight at 4°C. Subsequently, the sections were incubated with fluorescent secondary antibody at room temperature for 1 h and observed under a fluorescence microscope (Olympus IX73; Olympus Corporation). The fluorescence intensities were analyzed using ImageJ 1.51j8 (National Institutes of Health). The following primary antibodies were used: Anti-IL-1 β (1:100), anti-GFAP (1:100), anti-COX-2 (1:100) and anti-NF- κ B (1:100).

Western blot analysis. 6 h after the Res treatment, three rats were euthanized with an overdose of pentobarbital sodium (100~150 mg/kg) by intraperitoneal injection and sacrificed through decapitation. Lumbar spinal cord samples were collected and homogenized in RIPA lysis buffer containing 1% protease inhibitors (Sigma-Aldrich; Merck KGaA). After centrifugation at 12,000 g, 4°C for 20 min, the supernatant was collected. For cells, after treatment, the cells in the cell

culture dish were collected in a centrifuge tube. The cells were lysed in ice-cold RIPA buffer, after cell lysis, one third volume of 4x sample loading buffer was added and heated in boiling water bath for 10 min and ultrasonic treatment of 10~15 sec. After centrifugation at 12,000 g, 4°C for 20 min, the supernatant was collected. Protein concentration (tissue and cells) was quantified using a BCA analysis kit (Beyotime Biotechnology). Protein lysates (40 μ g/lane) were separated on 10% SDS-PAGE and transferred to 0.22 μ m PVDF membranes. Membranes were blocked with 5% milk in TBST (0.1% Tween-20) for 1 h at room temperature. Then the membranes were incubated with specific primary antibodies at 4°C overnight and HRP-conjugated secondary antibodies in TBST (1:5,000) at room temperature for 1 h. Protein bands were visualized using ECL detection reagent (Biosharp Life Sciences) and detected with an iBright 1500 instrument (Invitrogen; Thermo Fisher Scientific, Inc.). The grey values of western blot bands were analyzed using ImageJ 1.51j8 software (National Institutes of Health). β -actin was used as a loading control. The following primary antibodies were used: Anti-IL-1 β (1:1,000), anti-GFAP (1:1,000), anti-COX-2 (1:1,000), anti-NF- κ B (1:1,000), anti-TNF- α (1:1,000) and anti- β -actin (1:1,000).

Reactive oxygen species (ROS) assessment. Reactive Oxygen Species Assay Kit uses fluorescent probe DCFH-DA for ROS detection. The DCFH-DA was diluted with serum-free medium at 1:1,000 to a final concentration of 10 μ M. The cell culture medium was removed and diluted DCFH-DA was added. Cells were incubated at 37°C for 30 min. After incubation, cells were washed three times with serum-free medium to adequately remove DCFH-DA that did not enter the cell. Then the cells were placed under a fluorescence microscope (Olympus IX73; Olympus) for observation. The fluorescence intensities were analyzed using ImageJ 1.51j8 software.

Mitochondrial membrane potential detection. Following Res treatment, the cell culture medium is removed and the Mito-Tracker Red CMXRos working solution was added, and the cells are incubated at 37°C for 20 min. Then the Mito-Tracker Red CMXRos working solution was removed and the fresh cell culture medium was added. The cells were observed by fluorescence microscope (Olympus IX73; Olympus). The fluorescence intensities were analyzed using ImageJ 1.51j8 software (National Institutes of Health).

Molecular docking. The X-ray crystal structure of COX-2 was obtained from the Protein Data Bank (PDB ID: 5f19; rcsb.org/structure/5F19). The structure of Res was downloaded from the PubChem database (pubchem.ncbi.nlm.nih.gov/compound/445154) and optimized using ChemBio3D Ultra 14.0 software (PerkinElmer Informatics). Auto Dock Vina 1.2.0 software (Center For Computational Structural Biology) was used to dock conformation between COX-2 and Res. PyMOL 2.2.3 (PyMOL by Schrödinger, DeLano Scientific LLC; pymol.org/installers/) was used to visualize the conformation.

Statistical analysis. All statistical analyses were performed using SPSS 21.0 statistics software (IBM Corp.). Data obtained through H&E staining, immunofluorescence and

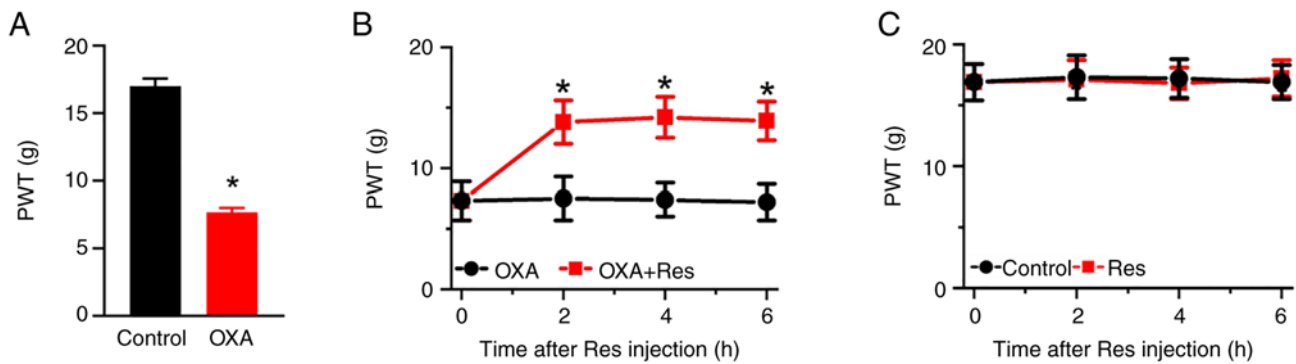


Figure 1. Res treatment alleviates OXA-induced neuropathic pain. (A) PWT values of rats in the Control and OXA groups after 5 days of OXA induction. Data are presented as the mean \pm SEM (n=6). *P<0.05 vs. Control. Effect of Res treatment on PWT values in (B) OXA and OXA + Res and (C) Control and Res groups. Data are presented as the mean \pm SEM (n=6). *P<0.05 vs. OXA. PWT, paw withdrawal threshold; OXA, oxalipatin; Res, resveratrol.

western blotting were analyzed using one-way analysis of variance followed by Tukey's test and presented as the mean \pm SD. PWT data were analyzed using unpaired Student's t-test and presented as the mean \pm SEM. P<0.05 was considered to indicate a statistically significant difference. All the experiments were repeated three times.

Results

Res treatment relieves OXA-induced mechanical allodynia.

To investigate the effect of Res on neuropathic pain, an OXA-induced neuropathic pain rat model was established by once-daily intraperitoneal injection of OXA for 5 consecutive days. On day 6 after the OXA administration, the PWT value indicating mechanical pain sensitivity was recorded. The PWT values in the OXA group were significantly decreased compared with those in the Control group (P<0.05; Fig. 1A). The PWT values of the Control and OXA groups were 17.0 \pm 0.6 and 7.7 \pm 0.3, respectively. Res was intrathecally injected into the lumbar spinal cord of OXA rats. The PWT values of OXA-induced rats were significantly increased at 2-6 h after Res treatment (Fig. 1B). The PWT values of the OXA and OXA + Res groups at post-treatment time points of 2, 4 and 6 h were 7.5 \pm 1.8 vs. 13.8 \pm 1.8 (P<0.05 vs. OXA group), 7.4 \pm 1.4 vs. 14.2 \pm 1.7 (P<0.05 vs. OXA group) and 7.2 \pm 1.5 vs. 13.9 \pm 1.6 (P<0.05 vs. OXA group), respectively. However, Res treatment had no significant effect on the mechanical pain behavior of control rats (Fig. 1C).

Res decreases OXA-induced spinal inflammation. Histological characterization was performed to analyze spinal inflammation. Subsequent to OXA administration, severe infiltration of inflammatory cells (red arrow) was observed in the spinal dorsal horn, while Res treatment decreased the inflammatory response induced by OXA administration (Fig. 2A). The relative inflammation scores in the OXA and OXA + Res groups were 2.9 \pm 0.03 (P<0.05 vs. Control; Fig. 2C) and 2.5 \pm 0.04 (P<0.05 vs. OXA group; Fig. 2C), respectively. Pro-inflammatory cytokines, such as TNF- α and IL-1 β , promote the inflammatory reaction and are associated with the process of pathological pain (26). OXA enhanced the fluorescence intensities of spinal IL-1 β , while this increase was reduced by Res treatment (Fig. 2B). The relative intensities

of the OXA and OXA + Res groups were 1.28 \pm 0.06 (P<0.05 vs. Control) and 1.06 \pm 0.09 (P<0.05 vs. OXA group; Fig. 2D), respectively. Western blot analysis indicated upregulation of spinal TNF- α and IL-1 β protein expression in the OXA group (Fig. 2E). The relative gray values of TNF- α and IL-1 β in the OXA group were 2.24 \pm 0.09 and 1.84 \pm 0.02, respectively (P<0.05 vs. Control; Fig. 2F). Following Res treatment, the levels of TNF- α and IL-1 β were decreased to 1.59 \pm 0.02 and 1.32 \pm 0.04, respectively (P<0.05 vs. OXA group; Fig. 2F).

Res inhibits spinal astrocyte activation. Localization, distribution and expression of the astrocytic marker GFAP were measured using an immunofluorescence assay and western blot analysis. The fluorescence intensity of spinal GFAP was increased in the OXA group, while it was decreased in the OXA + Res group compared with the Control group (Fig. 3A). The relative fluorescence intensities of the OXA and OXA + Res groups were 1.23 \pm 0.05 (P<0.05 vs. Control; Fig. 3B) and 0.86 \pm 0.09 (P<0.05 vs. OXA group; Fig. 3B), respectively. Western blot analysis indicated that relative GFAP expression was increased to 1.70 \pm 0.01 in the OXA group (P<0.05 vs. Control; Fig. 3C and D), whereas Res treatment reduced the relative spinal GFAP expression in the OXA + Res group with the relative grey value decreased to 0.63 \pm 0.01 (P<0.05 vs. OXA group; Fig. 3C and D).

Res reduces COX-2 expression. COX-2 is involved in inflammatory responses and COX-2 inhibitors are used as nonsteroidal anti-inflammatory drugs (22). To identify if Res is a potential COX-2 inhibitor, a molecular docking assay was performed on the X-ray crystal structures of COX-2 and the ligand Res (Fig. 4A-C). Auto Dock data showed that Res formed six hydrogen bonds with COX-2 at residues H39, R44, D125 and G135. H39 and R44 belong to the epidermal growth factor-like domain of COX-2 and D125 and G135 belong to the C-terminal globular catalytic domain of COX-2. An immunofluorescence assay and western blot analysis were used to detect spinal COX-2 location and expression, respectively. The fluorescence intensity of spinal COX-2 was increased in the OXA group with a relative fluorescence intensity of 1.26 \pm 0.08 (P<0.05 vs. Control; Fig. 4D and E). Res exerted an inhibitory effect on COX-2 expression, which showed a relative fluorescence intensity of 0.93 \pm 0.09 (P<0.05 vs. OXA; Fig. 4D and E).

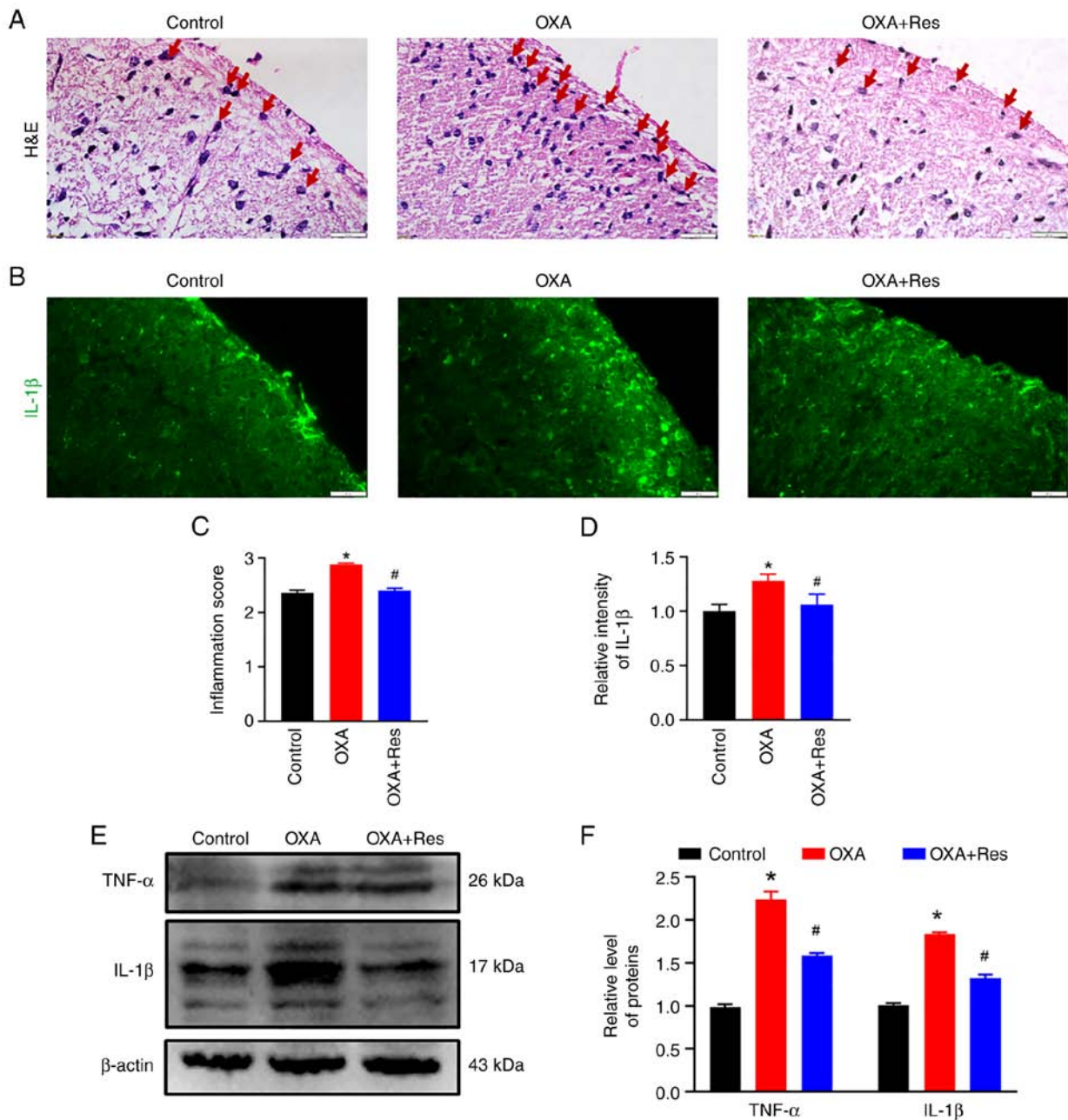


Figure 2. Res treatment decreases the OXA-induced spinal inflammatory response. (A) Representative images of H&E staining of spinal cord sections from the Control, OXA and OXA + Res groups (scale bar, 20 μ m). (B) Representative IL-1 β immunofluorescence staining images of spinal cord sections from Control, OXA and OXA + Res groups (scale bar, 20 μ m). (C) Relative inflammation score of Control, OXA and OXA + Res groups. (D) Quantitative data analysis of IL-1 β fluorescence intensity shown as the mean \pm SD (n=3). *P<0.05 vs. Control. #P<0.05 vs. OXA. (E) Western blot analysis of the expression levels of TNF- α and IL-1 β in spinal cord of the Control, OXA and OXA + Res groups. (F) Semi-quantitative data analysis of TNF- α and IL-1 β levels presented as the mean \pm SD (n=3). *P<0.05 vs. Control. #P<0.05 vs. OXA. OXA, oxaliplatin; Res, resveratrol.

Western blot analysis indicated that COX-2 expression was upregulated in the OXA group (Fig. 4F) showing a relative gray value of 1.76 ± 0.03 (P<0.05 vs. Control; Fig. 4G). The present data indicated that spinal COX-2 was upregulated after OXA administration. The upregulated COX-2 expression was reduced following Res treatment (Fig. 4F) with a relative gray value decreased to 1.06 ± 0.04 (P<0.05 vs. OXA; Fig. 4G).

Res decreases NF- κ B expression. The effect of Res on NF- κ B was detected using an immunofluorescence assay and western blot analysis. The relative fluorescence intensity of spinal NF- κ B in the OXA group was significantly increased

to 1.45 ± 0.12 , while Res treatment in the OXA + Res group reduced the increase in relative fluorescence intensity to 1.17 ± 0.13 (P<0.05 vs. OXA; Fig. 5A and B). The relative expression levels of the spinal NF- κ B protein were significantly increased to 1.55 ± 0.02 in the OXA group (P<0.05 vs. Control; Fig. 5C and D), whereas these were significantly decreased to 1.12 ± 0.01 in the OXA + Res group compared with the OXA group (P<0.05; Fig. 5C and D).

Confirmation of the anti-inflammatory effect of Res in C6 cells. C6 rat glioma cells were treated with TNF- α to induce inflammation. Western blot analysis indicated an increase in COX-2

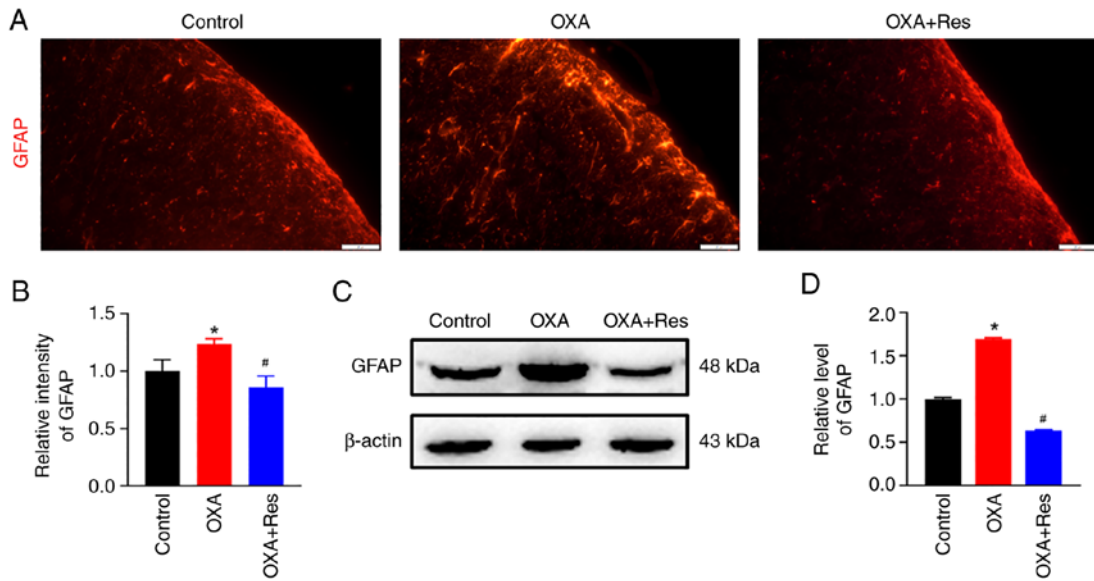


Figure 3. Res administration inhibits spinal astrocytic activation. (A) Representative immunofluorescence staining images of spinal GFAP in the Control, OXA and OXA + Res groups (scale bar, 20 μ m). (B) Quantitative data analysis of GFAP fluorescence intensity of spinal GFAP presented as the mean \pm SD (n=3). *P<0.05 vs. Control. #P<0.05 vs. OXA. (C) Western blot analysis of GFAP protein levels in the spinal cord of the Control, OXA and OXA + Res groups. (D) Semi-quantitative data analysis of GFAP levels presented as the mean \pm SD (n=3). *P<0.05 vs. Control. #P<0.05 vs. OXA. OXA, oxaliplatin; GFAP, glial fibrillary acidic protein; Res, resveratrol.

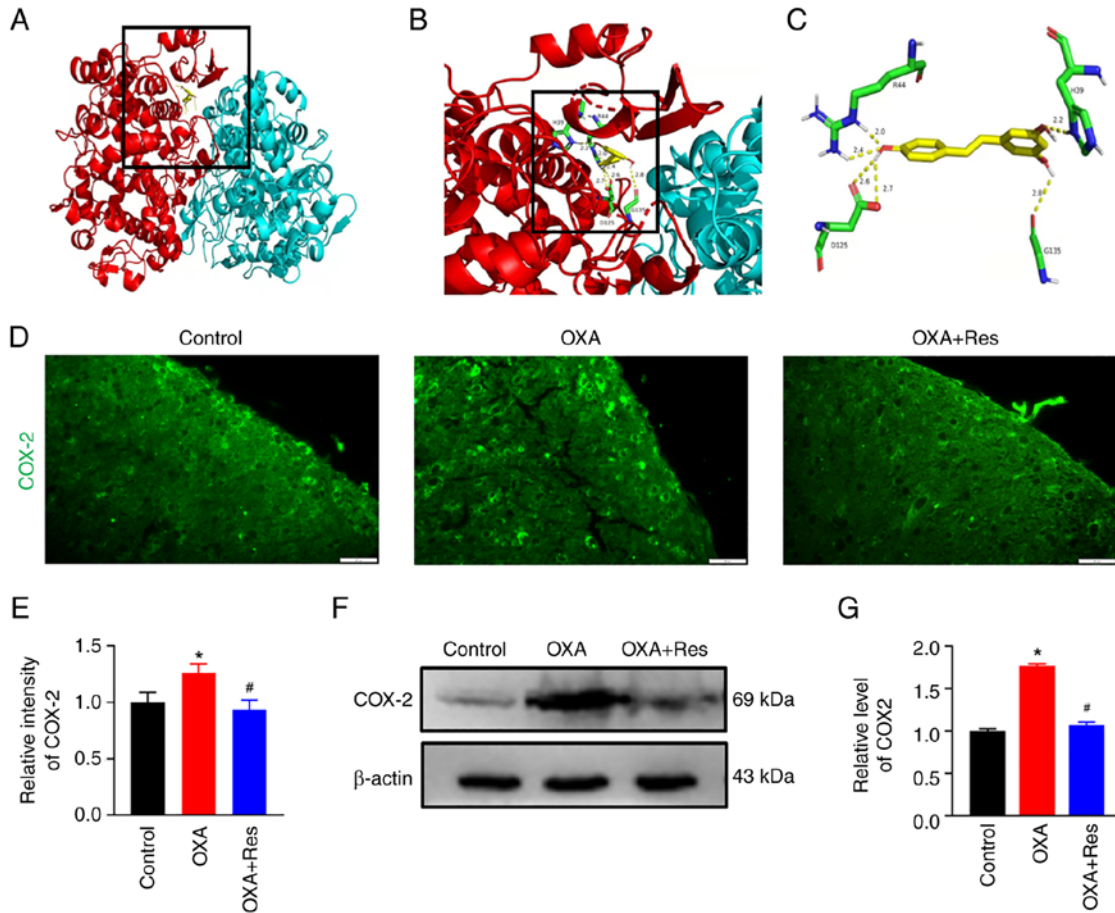


Figure 4. Res treatment reduces COX-2 expression. (A) 3D structure model of COX-2 docked with Res generated using Auto Dock. (B) Enlarged view of the binding site in the box. (C) Detail of the COX-2/Res interaction. COX-2 is shown in red and cyan, and Res is shown in yellow. The interaction bonds are shown as yellow dotted lines and the numbers represent the bond lengths. (D) Representative images of immunofluorescence staining of COX-2 in the spinal cord section of the Control, OXA and OXA + Res groups (scale bar, 20 μ m). (E) Quantitative data analysis of COX-2 fluorescence intensity presented as the mean \pm SD (n=3). *P<0.05 vs. Control. #P<0.05 vs. OXA. (F) Western blot analysis of expression levels of spinal COX-2 in the Control, OXA and OXA + Res groups. (G) Semi-quantitative data analysis of COX-2 expression presented as the mean \pm SD (n=3). *P<0.05 vs. Control. #P<0.05 vs. OXA. COX-2, cyclooxygenase-2; OXA, oxaliplatin; Res, resveratrol.

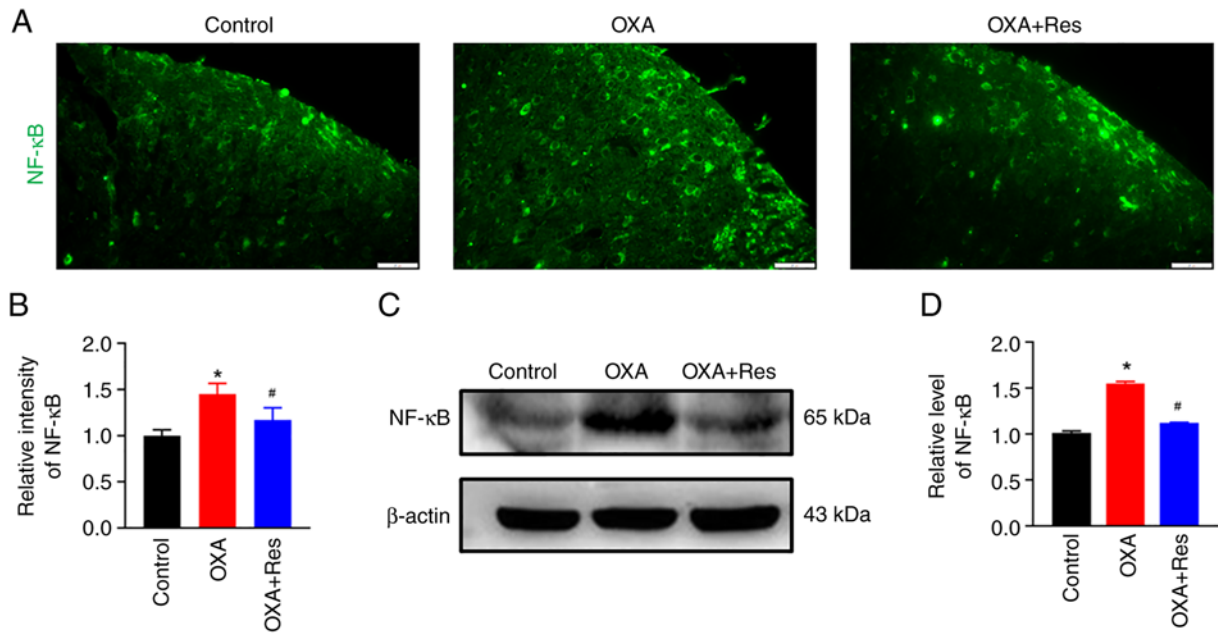


Figure 5. Res treatment decreases NF-κB expression. (A) Representative immunofluorescence staining images of spinal NF-κB in the Control, OXA and OXA + Res groups (scale bar, 20 μm). (B) Quantitative data analysis of NF-κB fluorescence intensity presented as the mean ± SD (n=3). *P<0.05 vs. Control. #P<0.05 vs. OXA. (C) Western blot analysis of NF-κB in the spinal cord of Control, OXA and OXA + Res groups. (D) Semi-quantitative data analysis of NF-κB expression presented as the mean ± SD (n=3). *P<0.05 vs. Control. #P<0.05 vs. OXA. OXA, oxaliplatin; Res, resveratrol.

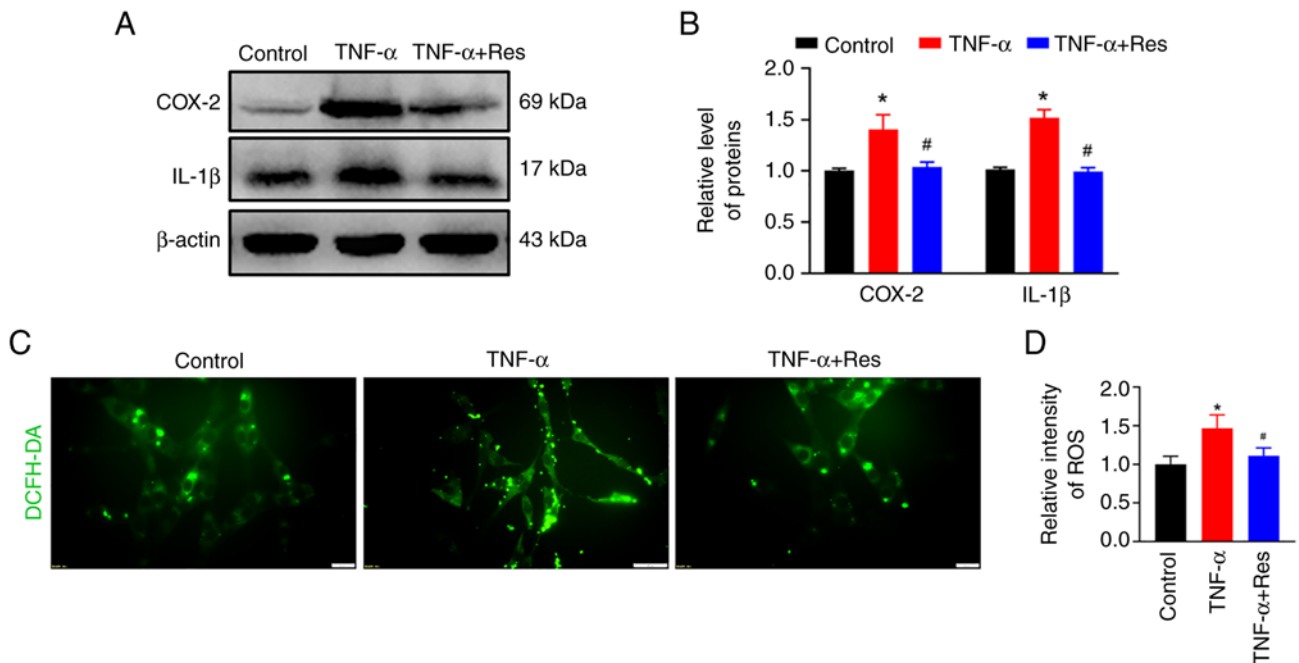


Figure 6. Effect of Res on the levels of inflammatory factors and ROS production in C6 cells. (A) Western blot analysis of expression levels of COX-2 and IL-1β in the Control, TNF-α and TNF-α + Res groups. (B) Semi-quantitative data analysis of COX-2 and IL-1β expression presented as the mean ± SD (n=3). *P<0.05 vs. Control. #P<0.05 vs. TNF-α. (C) Change in ROS detected in the Control, TNF-α and TNF-α + Res groups. (D) Quantitative analysis of the relative ROS generation presented as the mean ± SD (n=3). *P<0.05 vs. Control. #P<0.05 vs. TNF-α. COX-2, cyclooxygenase-2; DCFH-DA, 2,7-Dichlorodi-hydrofluorescein diacetate; Res, resveratrol; ROS, reactive oxygen species.

and IL-1β expression in TNF-α-treated cells that was significantly reduced in the TNF-α + Res group (Fig. 6A). The relative expression levels of COX-2 and IL-1β in the TNF-α-treated group were 1.49 ± 0.32 and 1.51 ± 0.08 , respectively ($P < 0.05$ vs. Control; Fig. 6B), while in the TNF-α + Res group these were 1.04 ± 0.05 and 0.99 ± 0.04 , respectively ($P < 0.05$ vs. TNF-α;

Fig. 6B). The ROS production marked by DCFH-DA was used to analyze the effect of Res on ROS production. Res treatment reduced the TNF-α-induced high ROS levels (Fig. 6C) and the relative ROS fluorescence intensities in the TNF-α and TNF-α + Res groups were 1.47 ± 0.17 ($P < 0.05$ vs. Control; Fig. 6D) and 1.11 ± 0.10 ($P < 0.05$ vs. TNF-α; Fig. 6D), respectively.

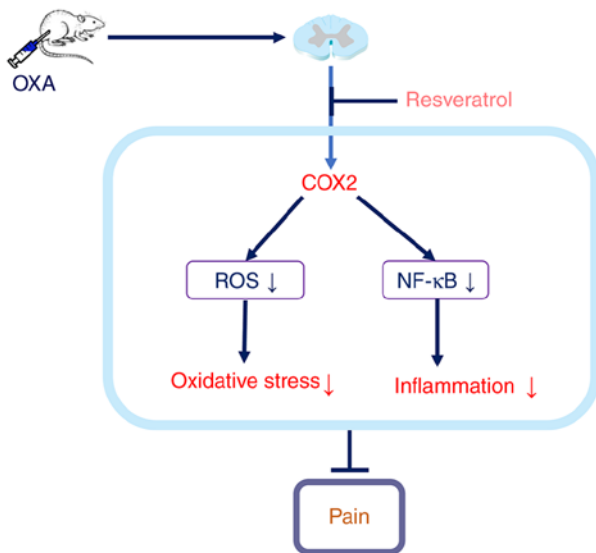


Figure 7. Schematic of the underlying mechanism of action of resveratrol in reducing spinal inflammation and reversing OXA-induced neuropathic pain. OXA, oxaliplatin; ROS, reactive oxygen species; COX-2, cyclooxygenase-2.

The present results demonstrated that intrathecal injection of Res inhibited COX-2 expression, reduced high ROS levels, decreased spinal inflammation and relieved OXA-induced neuropathic pain (Fig. 7).

Discussion

According to the global cancer statistics produced by the International Agency for Research on Cancer, there are ~19.3 million new cancer cases and ~10.0 million cancer deaths worldwide in 2020. Among them, ~4.57 million new cancer cases occurred in China, accounting for 23.7% of the cancer cases worldwide, ranking first in the world (27). Chemotherapy is a type of drug treatment used in numerous types of cancer to kill cancer cells and shrink tumor size. OXA is a platinum-based chemotherapeutic drug used to treat several types of cancer and has certain commonly reported side effects, including peripheral neuropathy (2,28). OXA-induced neuropathy is manifested following multiple chemotherapy cycles and is characterized by paresthesia and pain (29,30). The severity of this condition may require a reduction in the dose of OXA or even discontinuation of OXA chemotherapy, which is unfavorable for tumor control and survival (31). In the present study, once-daily intraperitoneal injection of OXA for 5 consecutive days in rats increased pain sensitivity, spinal inflammation reaction and oxidative stress. This suggested that spinal cord inflammation and increased oxidative stress were involved in the OXA-induced neuropathic pain. OXA is considered to upregulate oxidative stress-related genes (32) and induce overproduction of free radicals, such as ROS (33). COX-2 is an important enzyme that is involved in free radical scavenging (34). In the present study, the spinal COX-2 protein expression was upregulated following OXA treatment.

Spinal cord inflammation, a cardinal feature of pain, is characterized by activated glial cells and increased production of inflammatory mediators (35). TNF- α and IL-1 β are the

most potent and studied inflammatory cytokines expressed in the microglia cells and astrocytes of the spinal cord (36). NF- κ B is the main regulator of the inflammatory response by activating a variety of transcription factors, such as TNF- α and IL-1 β (37). In the present study, OXA administration induced the upregulation of the astrocytic marker GFAP, inflammation-related factor NF- κ B, TNF- α and IL-1 β . COX-2 operates by regulating NF- κ B signaling. Treatment with COX-2 inhibitor celecoxib decreases NF- κ B expression in a dose and time-dependent manner. Furthermore, COX-2 regulates E-cadherin expression through the NF- κ B/Snail signaling pathway in gastric cancer (38,39). Therefore, we hypothesized that COX-2 mediates the inflammatory process by regulating NF- κ B signaling.

Res has an antioxidant effect and, as a free radical scavenger, reduces the content of free radicals and inhibits the production of ROS (40). Through 3D molecular docking technology, the molecular structure of Res can be accurately linked to the molecular structure of COX-2, indicating that Res can target the site of COX action, thereby inhibiting epoxidation (41). Res can also reduce mitochondrial damage by regulating mitochondrial membrane potential, inhibiting mitochondrial lipid peroxidation and regulating mitochondrial gene expression (42). Mitochondrial function damage can cause a sharp rise in the level of ROS, thereby accelerating nerve cell apoptosis (43). In the present study, Res reduced ROS generation and the inflammatory reaction through the inhibition of COX-2. In conclusion, the present study revealed that intrathecal injection of Res could inhibit COX-2 expression, reduce ROS levels, decrease spinal inflammation and relieve OXA-induced neuropathic pain.

Acknowledgements

Not applicable.

Funding

The present study was supported by the National Natural Science Foundation of China (grant nos. 81971066, 81901149 and 32100823), Research Project of Hubei Provincial Department of Education (grant no. Q20212804) and Hubei University of Science and Technology Program (grant nos. 2020TD02 and BK202116).

Availability of data and materials

The datasets used and/or analyzed during the current study are available from the corresponding author on reasonable request.

Authors' contributions

ZBD, YJW, WJW, JW, BJW, HLZ, MX and LL performed experiments, collected and analyzed data and drafted the manuscript. ZBD and YJW confirm the authenticity of all the raw data. LL designed experiments, analyzed data and wrote the manuscript. All authors read and approved the final manuscript.

Ethics approval and consent to participate

All experimental procedures in the present study were performed in compliance with the local and international guidelines on ethical use of animals and all efforts were made to minimize the number of animals used and their sufferings. The animal experiments were approved by the Experimental Animal Ethics Committee of Hubei University of Science and Technology (approval no. 2020-01-900; Xianning, China).

Patient consent for publication

Not applicable.

Competing interests

The authors declare that they have no competing interests.

References

- Yi Y, Li L, Song F, Li P, Chen M, Ni S, Zhang H, Zhou H, Zeng S and Jiang H: L-tetrahydropalmatine reduces oxaliplatin accumulation in the dorsal root ganglion and mitochondria through selectively inhibiting the transporter-mediated uptake thereby attenuates peripheral neurotoxicity. *Toxicology* 459: 152853, 2021.
- Kang L, Tian Y, Xu S and Chen H: Oxaliplatin-induced peripheral neuropathy: Clinical features, mechanisms, prevention and treatment. *J Neurol* 268: 3269-3282, 2021.
- Takeshita E, Ishibashi K, Koda K, Oda N, Yoshimatsu K, Sato Y, Oya M, Yamaguchi S, Nakajima H, Momma T, *et al*: The updated five-year overall survival and long-term oxaliplatin-related neurotoxicity assessment of the FACOS study. *Surg Today* 51: 1309-1319, 2021.
- Furgała-Wojas A, Kowalska M, Nowaczyk A, Fijałkowski Ł and Sałat K: Comparison of bromhexine and its active metabolite-ambroxol as potential analgesics reducing oxaliplatin-induced neuropathic pain-pharmacodynamic and molecular docking studies. *Curr Drug Metab* 21: 548-561, 2020.
- Kong VKF and Irwin MG: Adjuvant analgesics in neuropathic pain. *Eur J Anaesthesiol* 26: 96-100, 2009.
- Tuttle AH, Tohyama S, Ramsay T, Kimmelman J, Schweinhardt P, Bennett GJ and Mogil JS: Increasing placebo responses over time in U.S. clinical trials of neuropathic pain. *Pain* 156: 2616-2626, 2015.
- Wang J, Zhang XS, Tao R, Zhang J, Liu L, Jiang YH, Ma SH, Song LX and Xia LJ: Upregulation of CX3CL1 mediated by NF- κ B activation in dorsal root ganglion contributes to peripheral sensitization and chronic pain induced by oxaliplatin administration. *Mol Pain* 13: 1744806917726256, 2017.
- Shigematsu N, Kawashiri T, Kobayashi D, Shimizu S, Mine K, Hiromoto S, Uchida M, Egashira N and Shimazoe T: Neuroprotective effect of alogliptin on oxaliplatin-induced peripheral neuropathy in vivo and in vitro. *Sci Rep* 10: 6734, 2020.
- Zhang P, Li X, Hu D, Lai Q, Wang Y, Ma X, Xu Q, Li W, Huang J and He J: Peripheral neural interface. *Adv Exp Med Biol* 1101: 91-122, 2019.
- Zhang X, Guan Z, Wang X, Sun D, Wang D, Li Y, Pei B, Ye M, Xu J and Yue X: Curcumin alleviates oxaliplatin-induced peripheral neuropathic pain through inhibiting oxidative stress-mediated activation of NF- κ B and mitigating inflammation. *Biol Pharm Bull* 43: 348-355, 2020.
- Menyhárt Á, Frank R, Farkas AE, Stüle Z, Varga VÉ, Nyúl-Tóth Á, Meiller A, Ivánkovits-Kiss O, Lemale CL, Szabó Í, *et al*: Malignant astrocyte swelling and impaired glutamate clearance drive the expansion of injurious spreading depolarization foci. *J Cereb Blood Flow Metab* 24: 271678X211040056, 2021.
- Li D, Liu N, Zhao HH, Zhang X, Kawano H, Liu L, Zhao L and Li HP: Interactions between Sirt1 and MAPKs regulate astrocyte activation induced by brain injury in vitro and in vivo. *J Neuroinflammation* 14: 67, 2017.
- Eto K, Kim SK, Takeda I and Nabekura J: The roles of cortical astrocytes in chronic pain and other brain pathologies. *Neurosci Res* 126: 3-8, 2018.
- Shaito A, Posadino AM, Younes N, Hasan H, Halabi S, Alhababi D, Al-Mohannadi A, Abdel-Rahman WM, Eid AH, Nasrallah GK and Pintus G: Potential adverse effects of resveratrol: A literature review. *Int J Mol Sci* 21: 2084, 2020.
- Salehi B, Mishra AP, Nigam M, Sener B, Kilic M, Sharifi-Rad M, Fokou PVT, Martins N and Sharifi-Rad J: Resveratrol: A double-edged sword in health benefits. *Biomedicines* 6: 91, 2018.
- Wilson T, Knight TJ, Beitz DC, Lewis DS and Engen RL: Resveratrol promotes atherosclerosis in hypercholesterolemic rabbits. *Life Sci* 59: PL15-PL21, 1996.
- Xu D, Li Y, Zhang B, Wang Y, Liu Y, Luo Y, Niu W, Dong M, Liu M, Dong H, *et al*: Resveratrol alleviate hypoxic pulmonary hypertension via anti-inflammation and anti-oxidant pathways in rats. *Int J Med Sci* 13: 942-954, 2016.
- Ma Y, Liu S, Shu H, Crawford J, Xing Y and Tao F: Resveratrol alleviates temporomandibular joint inflammatory pain by recovering disturbed gut microbiota. *Brain Behav Immun* 87: 455-464, 2020.
- Tao L, Ding Q, Gao C and Sun X: Resveratrol attenuates neuropathic pain through balancing pro-inflammatory and anti-inflammatory cytokines release in mice. *Int Immunopharmacol* 34: 165-172, 2016.
- Wang Y, Shi Y, Huang Y, Liu W, Cai G, Huang S, Zeng Y, Ren S, Zhan H and Wu W: Resveratrol mediates mechanical allodynia through modulating inflammatory response via the TREM2-autophagy axis in SNI rat model. *J Neuroinflammation* 17: 311, 2020.
- Hao M, Tang Q, Wang B, Li Y, Ding J, Li M, Xie M and Zhu H: Resveratrol suppresses bone cancer pain in rats by attenuating inflammatory responses through the AMPK/Drp1 signaling. *Acta Biochim Biophys Sin (Shanghai)* 52: 231-240, 2020.
- Ding H, Chen J, Su M, Lin Z, Zhan H, Yang F, Li W, Xie J, Huang Y, Liu X, *et al*: BDNF promotes activation of astrocytes and microglia contributing to neuroinflammation and mechanical allodynia in cyclophosphamide-induced cystitis. *J Neuroinflammation* 17: 19, 2020.
- Hylden JL and Wilcox GL: Intrathecal morphine in mice: A new technique. *Eur J Pharmacol* 67: 313-316, 1980.
- Luo H, Liu L, Zhao JJ, Mi XF, Wang QJ and Yu M: Effects of oxaliplatin on inflammation and intestinal floras in rats with colorectal cancer. *Eur Rev Med Pharmacol Sci* 24: 10542-10549, 2020.
- Song S, Guo R, Mehmood A, Zhang L, Yin B, Yuan C, Zhang H, Guo L and Li B: Liraglutide attenuate central nervous inflammation and demyelination through AMPK and pyroptosis-related NLRP3 pathway. *CNS Neurosci Ther* 28: 422-434, 2022.
- Matsuda M, Huh Y and Ji RR: Roles of inflammation, neurogenic inflammation, and neuroinflammation in pain. *J Anesth* 33: 131-139, 2019.
- Sung H, Ferlay J, Siegel RL, Laversanne M, Soerjomataram I, Jemal A and Bray F: Global cancer statistics 2020: GLOBOCAN estimates of incidence and mortality worldwide for 36 cancers in 185 countries. *CA Cancer J Clin* 71: 209-249, 2021.
- Austin PJ, Wu A and Moalem-Taylor G: Chronic constriction of the sciatic nerve and pain hypersensitivity testing in rats. *J Vis Exp* 13: 3393, 2012.
- Forstenpointner J, Oberlojer VC, Naleschinski D, Höper J, Helfert SM, Binder A, Gierthmühlen J and Baron R: A-fibers mediate cold hyperalgesia in patients with oxaliplatin-induced neuropathy. *Pain Pract* 18: 758-767, 2018.
- Lee JH and Kim W: The role of satellite glial cells, astrocytes and microglia in oxaliplatin-induced neuropathic pain. *Biomedicines* 8: 324, 2020.
- DiAntonio A: Axon degeneration: Mechanistic insights lead to therapeutic opportunities for the prevention and treatment of peripheral neuropathy. *Pain* 160 (Suppl 1): S17-S22, 2019.
- Lu Y, Lin Y, Huang X, Wu S, Wei J and Yang C: Oxaliplatin aggravates hepatic oxidative stress, inflammation and fibrosis in a non-alcoholic fatty liver disease mouse model. *Int J Mol Med* 43: 2398-2408, 2019.
- Agnes JP, Santos VW, das Neves RN, Gonçalves RM, Delgobo M, Girardi CS, Lückemeyer DD, Ferreira MA, Macedo-Júnior SJ, Lopes SC, *et al*: Antioxidants improve oxaliplatin-induced peripheral neuropathy in tumor-bearing mice model: Role of spinal cord oxidative stress and inflammation. *J Pain Aug* 22: 996-1013, 2021.
- Amić A, Marković Z, Marković JM, Jeremić S, Lučić B and Amić D: Free radical scavenging and COX-2 inhibition by simple colon metabolites of polyphenols: A theoretical approach. *Comput Biol Chem* 65: 45-53, 2016.

35. Hellenbrand DJ, Quinn CM, Piper ZJ, Morehouse CN, Fixel JA and Hanna AS: Inflammation after spinal cord injury: A review of the critical timeline of signaling cues and cellular infiltration. *J Neuroinflammation* 18: 284, 2021.
36. Teixeira-Santos L, Albino-Teixeira A and Pinho D: Neuroinflammation, oxidative stress and their interplay in neuropathic pain: Focus on specialized pro-resolving mediators and NADPH oxidase inhibitors as potential therapeutic strategies. *Pharmacol Res* 162: 105280, 2020.
37. Gebremedhn EG, Shortland PJ and Mahns DA: The incidence of acute oxaliplatin-induced neuropathy and its impact on treatment in the first cycle: A systematic review. *BMC Cancer* 18: 410, 2018.
38. Carothers AM, Davids JS, Damas BC and Bertagnolli MM: Persistent cyclooxygenase-2 inhibition downregulates NF- κ B, resulting in chronic intestinal inflammation in the min/+ mouse model of colon tumorigenesis. *Cancer Res* 70: 4433-4442, 2010.
39. Chen Z, Liu M, Liu X, Huang S, Li L, Song B, Li H, Ren Q, Hu Z, Zhou Y and Qiao L: COX-2 regulates E-cadherin expression through the NF- κ B/Snail signaling pathway in gastric cancer. *Int J Mol Med* 32: 93-100, 2013.
40. Song Q, Feng YB, Wang L, Shen J, Li Y, Fan C, Wang P and Yu SY: COX-2 inhibition rescues depression-like behaviors via suppressing glial activation, oxidative stress and neuronal apoptosis in rats. *Neuropharmacology* 160: 107779, 2019.
41. Meng T, Xiao D, Muhammed A, Deng J, Chen L and He J: Anti-inflammatory action and mechanisms of resveratrol. *Molecules* 26: 229, 2021.
42. Shamsara J and Shahir-Sadr A: Developing a CoMSIA Model for Inhibition of COX-2 by resveratrol derivatives. *Iran J Pharm Res* 15: 459-469, 2016.
43. Ito J, Shirasuna K, Kuwayama T and Iwata H: Resveratrol treatment increases mitochondrial biogenesis and improves viability of porcine germinal-vesicle stage vitrified-warmed oocytes. *Cryobiology* 93: 37-43, 2020.



This work is licensed under a Creative Commons Attribution-NonCommercial-NoDerivatives 4.0 International (CC BY-NC-ND 4.0) License.